forests

MDPI

Article

Identification, Classification and Characterization of bZIP Transcription Factor Family Members in *Pinus massoniana* Lamb.

Mengyang Zhang †, Peihuang Zhu †, Romaric Hippolyte Agassin, Sheng Yao, Dengbao Wang, Zichen Huang, Chi Zhang, Qingqing Hao and Kongshu Ji *

State Key Laboratory of Tree Genetics and Breeding, Co-Innovation Center for Sustainable Forestry in Southern China, Nanjing Forestry University, Nanjing 210037, China
* Correspondence: ksji@njfu.edu.cn
† These authors contributed equally to this work.

Abstract: Basic leucine zipper (bZIP) transcription factors (TFs) are ubiquitous in eukaryotes. Members of this family play significant roles in the regulation of plant growth, signal transduction, and various stresses. To date, bZIP TFs have been extensively studied in various plants, but there is little information about them in *Pinus massoniana* Lamb. In this study, 55 bZIP TFs were identified based on data from four different *P. massoniana* transcriptomes, and a systematic analysis was performed. According to the phylogenetic results, *P. massoniana* bZIP TFs were divided into 11 groups. Each bZIP protein contained a highly conserved bZIP domain, and the numbers and types of motifs were similar in the same group. The PmbZIPs were nuclear localization proteins. Based on the pine wood nematode inoculation transcriptome, the transcriptional profiles revealed that 25 *PmbZIP* genes could respond to pine wood nematodes at different levels. Genes *PmbZIP3, PmbZIP4, PmbZIP8, PmbZIP20,* and *PmbZIP23* were selected to be upregulated in the process of inoculation with pine wood nematodes. These five genes had different expression levels in different tissues and were responsive to the related treatment conditions. Transcriptional activity analysis showed that PmbZIP3 and PmbZIP8 were transcriptional activators; PmbZIP4, PmbZIP20 and PmbZIP23 were transcriptional repressors. These findings provide preliminary information on PmbZIP TFs, which is helpful for further study of other physiological functions of bZIP TFs in *P. massoniana*.

Keywords: *Pinus massoniana*; bZIP; stress response; hormone; expression pattern

Citation: Zhang, M.; Zhu, P.; Agassin, R.H.; Yao, S.; Wang, D.; Huang, Z.; Zhang, C.; Hao, Q.; Ji, K. Identification, Classification and Characterization of bZIP Transcription Factor Family Members in *Pinus massoniana* Lamb. *Forests* **2023**, *14*, 155. https://doi.org/10.3390/f14010155

Academic Editor: Rita Lourenço Costa

Received: 13 December 2022
Revised: 10 January 2023
Accepted: 11 January 2023
Published: 14 January 2023

1. Introduction

Transcription factors (TFs) are important regulators, also called *trans*-acting factors, that can combine with *cis*-acting elements in promoter regions, inhibiting or activating the transcription of target genes [1]. By regulating transcription efficiency, plants can respond to various factors over time to regulate normal growth and deal with the external stresses of plants [2]. According to structural characteristics and functions, TFs can be divided into basic leucine zipper (bZIP), NAC, MYB, WRKY, AP2/ERF families, and so on [3–6]. Among these families, the bZIP family is one of the most abundant [7].

The bZIP TFs are recognized by a bZIP conserved domain, which includes two important regions, namely, a basic region and a leucine zipper region [8]. The basic region is highly conservative and contains an N-X7-R/K structure, which helps to bind DNA sequences and preferentially binds to elements containing ACGT [9,10]. The leucine zipper region is less conservative and contains several repeats of leucine or other hydrophobic amino acids [11].

The bZIP TFs have been identified in many plant species, for example, *Ziziphus jujube* Mill. [12], *Vitis vinifera* L. [13], *Malus domestica* (Suckow) Borkh. [14], *Arabidopsis thaliana* (L.) Heynh. [7], and *Oryza sativa* L. [15]. The bZIP family is involved in many processes in

different biological functions. Numerous members' functional characteristics have been determined. For instance, *AtbZIP59* (group I) participates in auxin-induced callus formation, plant regeneration and growth; in the same group, *AtbZIP29* is expressed in proliferative tissues [16,17]. *AtbZIP19* (Group F) can bind to Zn-deficient reaction elements (ZDREs), which makes plants adapt to Zn-deficient environmental conditions [18]. *AtbZIP60* (group K) plays a crucial regulatory role in endoplasmic reticulum (ER) stress, and the correct folding of proteins in the ER has an important influence on survival [19]. The bZIP TFs of Group D members of *Arabidopsis* can bind to TGACG elements; among these members, *TGA1* and *TGA4* participate in SA and other signaling molecule biosynthesis to induce the defense response to pathogens [20]. The expression of the *ZjbZIP10* gene is increased after salt treatment, indicating that *ZjbZIP10* may function in resistance to salt stress [12]. The *OsbZIP62* gene is involved in the abscisic acid (ABA) signaling pathway in *O. sativa* and can also improve drought stress resistance [15].

The bZIP TFs can also regulate related physiological processes by regulating the expression of related genes. For example, *DkbZIP5* overexpression in *Diospyros kaki* can promote the expression of the *DkMYB4* gene and lead to the accumulation of a large amount of procyanidins in calli; therefore, the scavenging ability of reactive oxygen radicals was improved in plants [21]. The *bZIP* genes (*HY5* and *HYH*) upregulate the expression of the downstream key gene *DFR*, which promotes anthocyanin accumulation and increases the cold resistance of *Arabidopsis* [22]. Relevant research has shown that TbbZIP1 TF positively regulates the expression of the *TbSRPP1* gene and affects the synthesis of natural rubber [23].

Pinus massoniana Lamb. is the main forest tree species in China and is widely used in the paper, construction, rosin, and other industries; it also has significant roles in windbreak, sand fixation, water conservation, and climate regulation [24]. Additionally, *P. massoniana* trees can secrete complex oleoresins that includes terpenoids, such as monoterpenoids, diterpenoids, and sesquiterpenoids, which are important secondary metabolites and barriers against insects and pathogens. The release of these substances is one of the most important conifer defenses against a variety of biotic and abiotic stresses [25–27]. Moreover, bZIP TFs play important roles in a variety of biological processes in plants [28]. Therefore, *P. massoniana* is a good species to explore regarding multiple response mechanisms, and the *bZIP* gene functions of *P. massoniana* are very valuable. At present, bZIP TFs have rarely been reported in *P. massoniana*. While whole-genome sequencing made the identification of bZIP TF families possible, in the case of *P. massoniana*, there are no genomic resources available. Therefore, we identified bZIP TFs based on the four transcriptomes of *P. massoniana* that inoculated with pine wood nematode, drought stress, CO_2 stress and young shoot in the laboratory. These transcriptomes include the biological processes of physiological, biotic, and abiotic stresses, which were analyzed in different time periods. On the basis of transcriptome data, 55 PmbZIP TFs were identified and analyzed using bioinformatics methods. In addition, the expression patterns of representative PmbZIPs were analyzed in different conditions. These analyses provide useful information for studying bZIP TF functions in *P. massoniana*.

2. Materials and Methods

2.1. Identification of PmbZIP TFs

To identify members of the bZIP TFs family contained in the transcriptomes of *P. massoniana*, the hidden Markov model (HMM) was built according to the bZIP domain (PF00170 and PF07716) from the Pfam (http://pfam.xfam.org/, accessed on 23 February 2022) database. Then, based on the transcriptomes, namely, *P. massoniana* inoculated with the pine wood nematode (SRA accession: PRJNA660087); that is, after inoculation for 0, 3, 10, 20, and 35 d, needles were collected for sequencing. The CO_2-treated transcriptome: After *P. massoniana* seedlings were treated with high CO_2 concentrations, the needles were collected at 0, 6, 12 and 24 h, and transcriptome sequencing was performed (SRA accession: PRJNA561037) [29]. Young shoot transcriptome (SRA accession: PRJNA655997), the buds

were taken from the tender stems without any treatment. Drought-treated transcriptome (SRA accession: PRJNA595650): The transcriptome controlled the soil moisture content in four gradients, normal, light, mild, and severe, by the weighing method; after treatment for 60 d, the needles were collected for sequencing. These transcriptomes were used to identify all contained PmbZIP TFs. The HMMER 3 program was used to screen, and the screening standard was set to $E < E^{-3}$. The protein sequences with more than 97% similarity in transcriptomes were deleted. Then, the bZIP TF domains were confirmed by Pfam and CD-search (https://www.ncbi.nlm.nih.gov/cdd/, accessed on 26 February 2022), and bZIP TFs with complete domains were chosen. The protein sequences and gene sequences can be found in Table S1 and Table S2, respectively. The ExPASy Proteomics Server (http://expasy.org/, accessed on 27 February 2022) website was used to predict the isoelectric point (pI), molecular weight (MW), amino acid (AA) number, and other physicochemical properties.

2.2. Conserved Domain and Phylogenesis Analysis of bZIP TFs

Sequence alignments of the PmbZIP protein conserved regions were performed by DNAMAN. *Arabidopsis thaliana* bZIP protein sequences were downloaded from the Plant Transcription Factor Database (http://planttfdb.cbi.pku.edu.cn/, accessed on 5 March 2022). Sequences of *P. massoniana* and *Arabidopsis* were aligned by the ClustalW program in MEGA 7.0 [30]. A phylogenetic tree was created by the maximum likelihood (ML) method, the verification parameter was the bootstrap, and the number of repetitions was 1000 [31]. Then, using EvolView (https://www.evolgenius.info/evolview/#login, accessed on 7 March 2022) software to edit the phylogenetic tree for visualization.

2.3. Examination of PmbZIP Protein Motifs

To determine the motifs distribution of PmbZIP proteins, the MEME (http://meme.nbcr.net/meme/, accessed on 14 March 2022) website was used to detect and obtain the motifs information; the number of motifs was set to 8, and the other parameters were default values. TBtools software was used to display the conserved motifs diagram [32].

2.4. Subcellular Localization

The subcellular localization of PmbZIP TFs was predicted by Cell-PLoc 2.0 (http://www.csbio.sjtu.edu.cn/bioinf/Cell-PLoc-2/, accessed on 18 October 2022). To confirm the predicted results, *PmbZIP4* and *PmbZIP20* were randomly chosen for subcellular localization experiment. The open reading frame (ORF) of *PmbZIP4* and *PmbZIP20* was obtained by gene cloning. The primers for gene cloning and vector construction are listed in Table S3. Inserting the ORF region without the stop codon into the pBI121-GFP vector, including green fluorescent protein (GFP), by recombinase, the 35S::PmbZIP4-GFP and 35S::PmbZIP20-GFP vectors were constructed. Subsequently, these vectors were transformed into *Agrobacterium* strain GV3101. The strains together with p19 (RNA silencing suppressor) *Agrobacterium* strain were cultured in LB medium at 28 °C for 36 h and suspended in injection solution (10 mM 2-(N-morpholino) ethanesulfonic acid (MES), 10 mM $MgCl_2$, 200 μM acetosyringone). Then, the suspension cells and p19 were mixed in 1:1 ratio, and the mixture was injected into *Nicotiana benthamiana* Domin leaves. The injected *N. benthamiana* plants were cultured with a 16 h light and 8 h dark photoperiod for 3 days. The GFP signal was captured via an LSM710 confocal microscope (Zeiss, Jena, Germany).

2.5. Transcriptional Pattern Analysis

The RNA sequencing (RNA-seq) data (SRA accession: PRJNA66087) were collected from the transcriptome of *P. massoniana* inoculated with the pine wood nematode to investigate the potential function of PmbZIPs in response to pine wood nematode inoculation, and the sequencing included five different time points (0, 3, 10, 20 and 35 d) after treatments. The expression levels were calculated by ascertaining the fragments per kilobase of transcript per million mapped reads (FPKM), and the FPKM values is provided in Table

S4. Finally, the transcript abundance of *PmbZIP* genes was converted to $\log_2$(FPKM + 1) values, and the expression heatmap was created via TBtools software [32].

2.6. Plant Materials and Treatments

Seeds of *P. massoniana* were obtained from the National Base of Improved Tree Species of *P. massoniana* of Xinyi, Guangdong, China. Two-year-old *P. massoniana* seedlings were transplanted into pots containing a soil mixture (peat: perlite: vermiculite, 3:1:1 (*v*/*v*)) at 24 °C with 16-h light and 8-h dark photoperiod. Seedlings with consistent growth status were used to subsequent experiments. To study the expression patterns of *PmbZIP* genes, four different tissues from the seedlings were taken, including roots, stems, mature needles, and young needles. Three seedlings with the same growth status were selected as three biological replicates. Expression in young needles was used as reference. Moreover, the seedlings were subjected to four treatments: 100 μM methyl jasmonate (MeJA), 500 μM ethephon (ETH), 1 mM salicylic acid (SA) and 10 mM H_2O_2. The seedling treatments were applied by spraying. For each treatment, we selected three seedlings with the same growth status as three biological replicates. The samples were collected at 0, 3, 12, and 24 h, and samples at 0 h were used as controls. Then, the collected samples were stored at −80 °C.

2.7. Quantitative Reverse Transcription PCR (qRT–PCR) Analysis of PmbZIP Genes

The samples were ground into powder with liquid nitrogen. Following the manufacturer's protocol, total RNA was extracted using an RNAprep Pure Kit (DP441, Tiangen Biotech, Beijing, China) combined with the gDNA removal step, and RNA purity and concentration were detected using the NanoDrop 2000 instrument (Thermo Fisher Scientific, Waltham, MA, USA). Then, cDNA (20 μL) was produced from 1000 ng total RNA using a first-strand cDNA synthesis kit (11141, Yeasen Biotech, Shanghai, China) according to the manufacturer's description. Primers were designed for qRT–PCR by Primer 5.0 (Table S3), and *TUA* (tubulin alpha) was used as an internal control [33]. Gene expression levels were measured via real-time fluorescence quantitative PCR technology, and PCR amplification was used with the StepOne system (Applied Biosystems, Foster City, CA, USA). The total volume was 10 μL, which comprised 5 μL of SYBR Green Real-time PCR Master Mix (QPK-201, Toyobo Bio-Technology, Shanghai, China), 1 μL of 20-fold diluted cDNA, 0.4 μL of each primer, and 3.2 μL of ddH_2O. The procedure was as follows: 95 °C for 2 min; 40 cycles at 95 °C for 10 s and 60 °C for 30 s; 95 °C for 15 s; and 60 °C for 1 min. Each reaction was repeated three times. Finally, gene expression levels were calculated by the $2^{-\Delta\Delta CT}$ method [34]. One-way analysis of variance (ANOVA) (Duncan's test) was analyzed using SPSS (IBM, New York, NY, USA).

2.8. Transcriptional Activity Assays

To investigate the transcriptional activation activity of PmbZIP proteins, the coding sequences of *PmbZIP3*, *PmbZIP4*, *PmbZIP8*, *PmbZIP20*, and *PmbZIP23* were integrated into the pGBKT7 vector digested by BamHI and NotI enzymes. Then, the products of ligation were transformed into *Escherichia coli* (*E. coli*) Trelief 5α competent cell and cultured at 37 °C. Single colonies were chosen for PCR amplification. The primers are listed in Table S3. Subsequently, the pGBKT7-PmbZIP recombinant plasmids with correctly sequencing were transferred into yeast competent cells AH109 and cultured on SD/-Trp medium for 3 d at 28 °C, single colonies of successfully transformed yeast strain were selected and cultured in SD/-Trp liquid medium. 5 μL of dilution incubated on SD/-Trp, SD/-Ade/-His/-Trp, and SD/-Ade/-His/-Trp containing X-α-gal solid medium for 3–5 d at 28 °C. After that, the growth status of yeast cells was observed and recorded.

3. Results

3.1. Identification of bZIP TF Sequences in P. massoniana

From the transcriptomes, 55 bZIP protein sequences were identified after removing repeat sequences and sequences without completely conserved domains. Then, the re-

maining TFs were renamed PmbZIP1-PmbZIP55. The 55 PmbZIP protein sequences were used for physicochemical property analysis (Table S5). The amino acid number ranged from 90 (PmbZIP52) to 771 (PmbZIP4), the molecular weight ranged from 10,698.33 (PmbZIP52) to 84,073.51 (PmbZIP4) Da, and the isoelectric point ranged from 4.88 (PmbZIP48) to 11.26 (PmbZIP37). In addition, the instability index (II) ranged from 27.53 (PmbZIP18) to 88.65 (PmbZIP52), and the aliphatic index ranged from 49.49 (PmbZIP54) to 82.94 (PmbZIP30). The number of amino acids and physicochemical properties varied greatly among different bZIP proteins. Moreover, the grand average of hydropathicity (GRAVY) was negative, indicating that these PmbZIP proteins were hydrophilic.

3.2. Conserved Domain Analysis of PmbZIP Proteins

To analyze the conserved characteristics of the predicted PmbZIP TFs, sequence alignments of the domains were performed (Figure 1). In the basic region, the core arginine (R) residue of the bZIP domain of only PmbZIP33 was substituted with a tryptophan (T) residue. Besides, all the remaining PmbZIP TF domains included an unchanged N-X7-R/K structure. Moreover, only PmbZIP1, PmbZIP6, PmbZIP10, and PmbZIP21 were N-X7-K residues. The remaining 51 PmbZIP TFs were N-X7-R residues, showing that lysine (K) was less conserved than arginine (R) in PmbZIP TFs. In the leucine zipper region, the first leucine (L) was highly conserved, except for PmbZIP26 and PmbZIP48, in which leucine was replaced by tryptophan (T) and alanine (A), respectively. Nevertheless, the following leucine was replaced more often than the first leucine; for example, the second leucine in PmbZIP5, PmbZIP29, PmbZIP32, PmbZIP36, PmbZIP43, PmbZIP45, and PmbIZP46 was replaced by methionine (M).

3.3. Phylogenetic Analysis of the bZIP TFs

To classify the evolutionary relationships of PmbZIP family members of *P. massoniana*, a phylogenetic tree was constructed including 126 bZIP proteins, namely, 55 bZIP proteins of *P. massoniana* and 71 bZIP proteins of *Arabidopsis*. Based on the classification of *A. thaliana*, the *P. massoniana* bZIPs were divided into 10 groups, namely, S, C, G, A, H, K, E, I, F, and D. In addition, we defined eight PmbZIPs as a new group of L (Figure 2). The evolutionary relationships showed that the grouping of bZIP TFs of *P. massoniana* was almost consistent with that of *A. thaliana*, indicating that the bZIP TFs of the two species were evolutionarily conserved. In addition, no PmbZIP TFs were found in groups J, B, or M, and in some groups, PmbZIP TFs and AtbZIP TFs were separately located together on a branch. For example, in group G, PmbZIP12, PmbZIP13, PmbZIP52, PmbZIP3, PmbZIP8 and PmbZIP14 were on a branch, while At1G32150.1, At2G35530.1, At2G46270.1, At4G01120.1 and At4G36730.1 were on another branch, indicating that there might be some differences in the evolutionary relationship of bZIP TFs among different species.

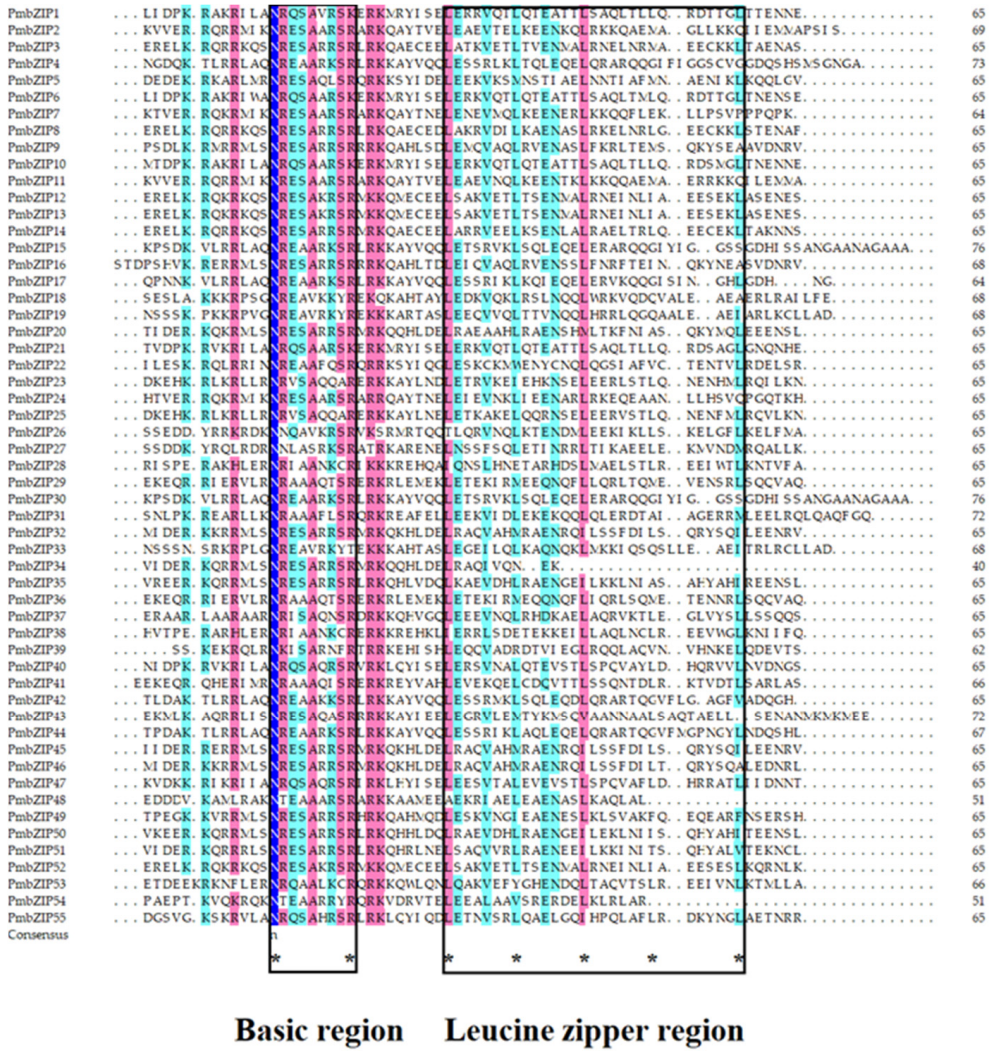

Figure 1. Sequence alignments of conserved domains of all bZIP family proteins in *P. massoniana* Lamb.. The dark blue, light red, and light blue backgrounds indicate protein identities of 100%, 75%, and 50%, respectively. The basic region and leucine zipper region are marked with black line boxes. The asterisks indicate the conserved amino acids of bZIP domain.

3.4. Motif Analysis of PmbZIP Proteins

Motif analysis further supports the reliability of the phylogenetic classification of PmbZIP TFs, and the conserved motifs were determined using the MEME website. Eight motifs were searched in the 55 PmbZIP proteins, which were named motifs 1–8. The motif sequences are shown in Table 1, and each motif sequence logo is generated in Figure S1. The amino acid number of the eight motifs varied from 11 to 50, and motifs 1 and 3 formed two main parts of the bZIP conserved domain. Motif 1 is a highly conserved N-X7-R/K structure with DNA recognition function and motif 3 is a less conserved leucine zipper structure, which is characterized by continuous α-helix [35]. The motif distribution of PmbZIP TFs is shown in Figure 3. All the proteins contained motif 1, and at the same time, most of the proteins included motif 3. The results showed that PmbZIP protein structures were complete.

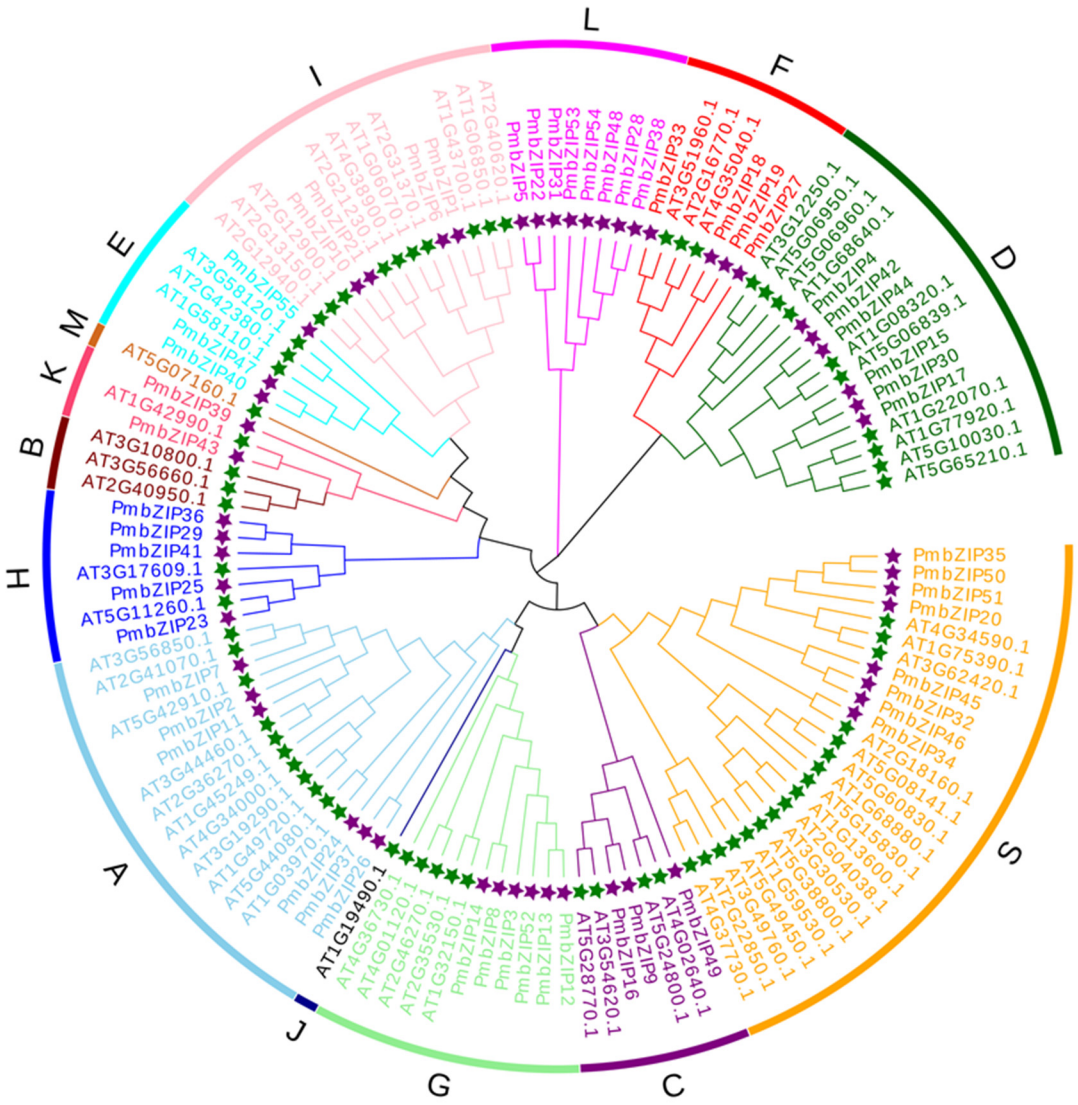

Figure 2. Phylogenetic tree of the bZIP TF family of *P. massoniana* and *A. thaliana*. The different color branches and surrounding letters represent different groups. The green stars represent AtbZIPs, and the purple stars represent PmbZIPs.

Table 1. Sequences of the motifs of PmbZIP TFs.

Motif	Length	Motif Sequence
1	22	LSNRESARRSRERKKAYLQELE
2	50	HYDELFRMKSVAAKADVFHLVSGMWKTPAERCFMWMG GFRPSELLKILVP
3	21	AKVAQLRAENTQLRKELTLLS
4	44	GAAAFDMEYARWLEEQHRQISDLRAALQAHVTDNEL RILVEGGM
5	34	VPPPPPYFASQVASGPTPHPYMWGGQPLMPPYGT
6	29	NVANYMGQMAMAMGKLGMLENFVHQADNL
7	11	KVIDERRQKRM
8	29	YTHGCTHTHTCNPPGPDNSHTHTCYHSLT

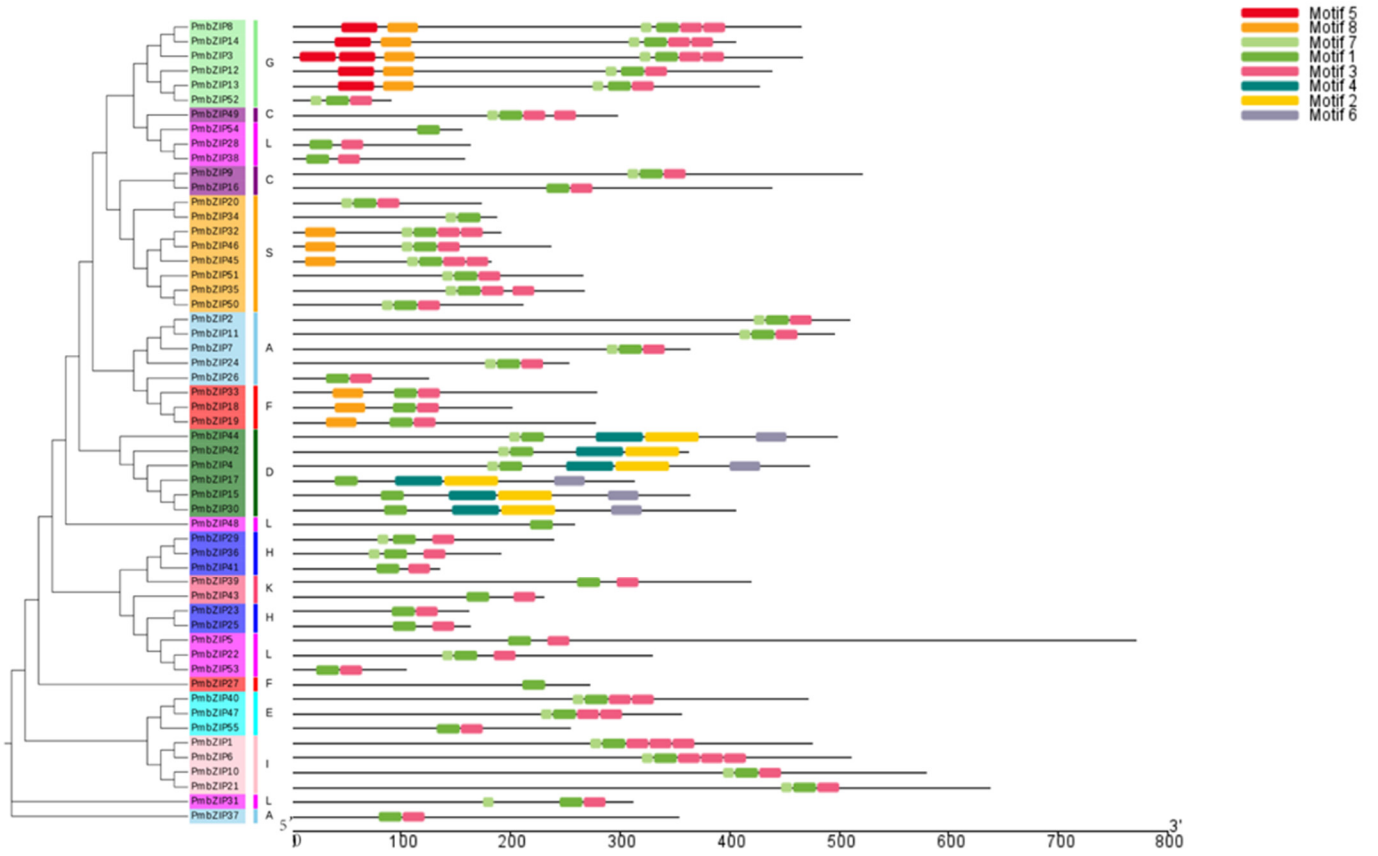

Figure 3. Motif analysis of the bZIP TFs in *P. massoniana*. The motif structures were obtained by MEME analysis. Eight conserved motifs of PmbZIP proteins are shown, and the different colors represent different kinds of motifs.

Additionally, in the same group, PmbZIP proteins generally contained similar numbers and types of motifs. For example, most members in group G contained not only motifs 1, 3, and 7 but also motifs 5 and 8. In addition, some motifs only existed in individual groups. For instance, motifs 6, 4, and 2 were identified only in group D members; motif 5 was found in group G members. The results indicated that the differences in motif distribution among different groups may reflect the differences in protein structure and some biological functions.

3.5. Subcellular Localization Analysis

The Cell-PLoc 2.0 prediction results showed that PmbZIP proteins were located in the nucleus (Table S6). To further comprehend the localization features of PmbZIPs, PmbZIP4 and PmbZIP20, were selected for the experiment. A fluorescent signal was found after transient transformation in tobacco leaves (Figure 4). The GFP signal was distributed throughout the whole cell in the control; however, GFP fused with PmbZIP4 and PmbZIP20 only showed fluorescence in the nucleus. The specific labelling of nuclei was also performed and that it did overlap with signal from GFP and GFP-labelled PmbZIPs (data not shown). The results indicated that these TFs are nuclear localization protein.

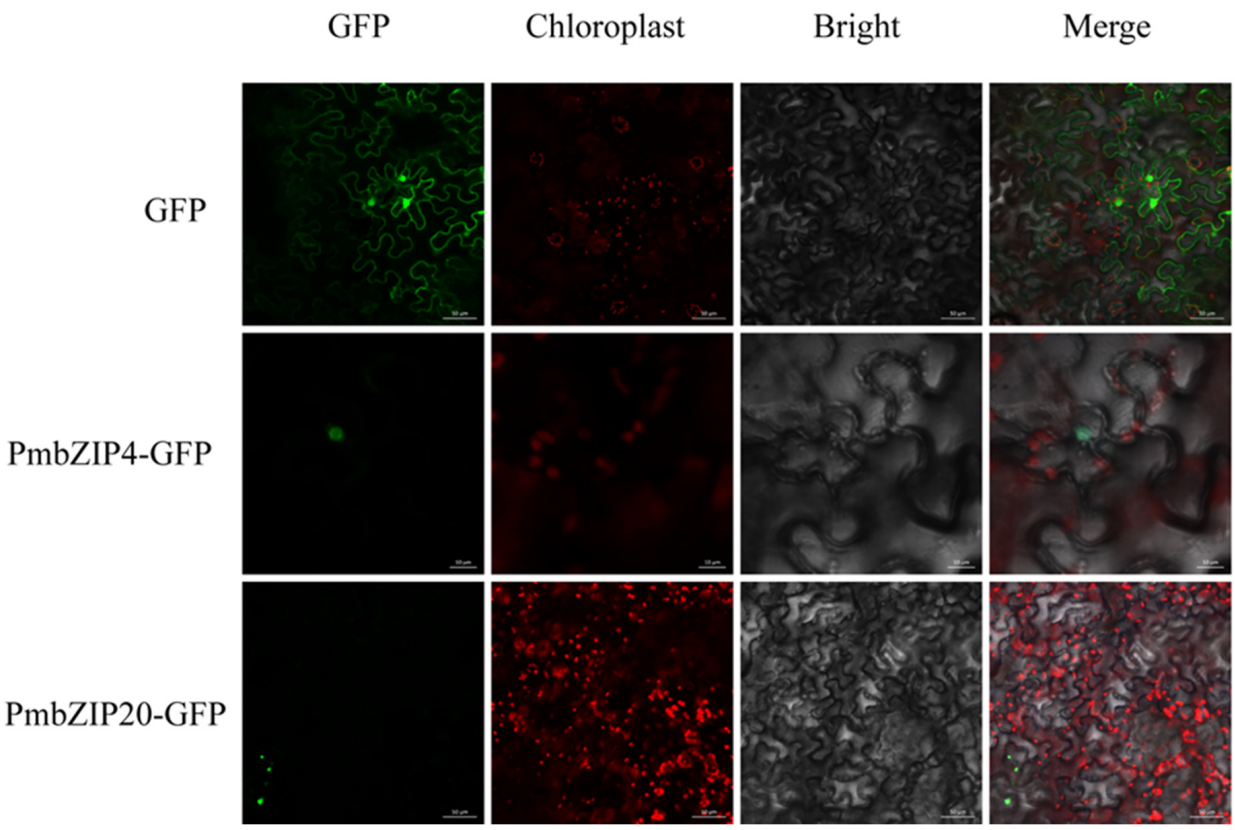

Figure 4. Subcellular localization analysis of PmbZIP4 and PmbZIP20 protein. Transient expression of GFP (control), PmbZIP4-GFP and PmbZIP20-GFP in *N. benthamiana* leaves. The scale in the images of GFP and PmbZIP20-GFP is 50 μM, and the scale in the images of PmbZIP4-GFP is 20 μM.

3.6. Transcriptional Profile Analysis of PmbZIP Genes

To investigate the potential role of *PmbZIPs* in response to pine wood nematode inoculation, we investigated the expression patterns of *PmbZIPs* based on the transcriptomic data (SRA accession: PRJNA66087), and an expression heatmap was constructed (Figure 5). The results showed that only *PmbZIP1-PmbZIP25* genes were detected and expressed in response to inoculation. These *PmbZIP* genes were up-regulated in varying degrees after inoculation. For example, the expression levels of *PmbZIP6*, *PmbZIP10*, *PmbZIP21*, *PmbZIP3*, *PmbZIP14* and *PmbZIP24* increased after inoculation for 3 d. The expression of *PmbZIP1*, *PmbZIP2*, *PmbZIP7*, *PmbZIP11*, *PmbZIP8*, *PmbZIP13*, *PmbZIP5*, *PmbZIP22*, and *PmbZIP16* increased after inoculation for 35 d. High-level expression of only *PmbZIP18* was detected after inoculation for 20 d. Moreover, some genes retained continuously high expression levels after inoculation. For instance, the expression of *PmbZIP23* was significantly increased at 10, 20, and 35 d. There was also a trend in which the expression levels of some genes, such as *PmbZIP4* and *PmbZIP20*, first increased, then decreased and subsequently increased. The results suggested that these *PmbZIP* genes responded to pine wood nematode infection.

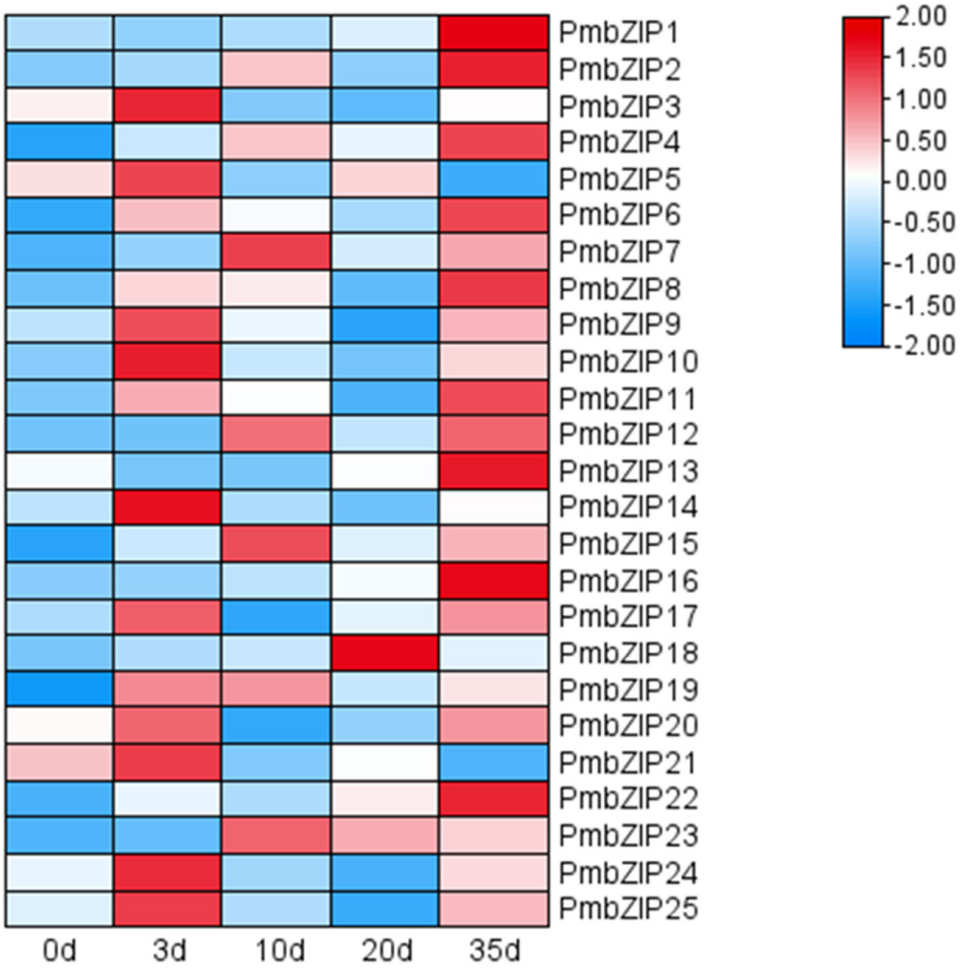

Figure 5. Transcriptional profiles of *PmbZIP* family members after inoculation with pine wood nematodes in *P. massoniana* corresponding to five stages: 0 (CK), 3, 10, 20, and 35 d. A heatmap was generated by the $\log_2$(FPKM + 1) value, and the color scale represents the relative expression level.

3.7. Expression Patterns of Selected PmbZIPs in Various Parts of the Plant

According to the transcriptional profile of *P. massoniana* inoculated with pine wood nematodes, five representative *PmbZIP* (*PmbZIP3*, *PmbZIP4*, *PmbZIP8*, *PmbZIP20*, *PmbZIP23*) genes with significantly up-regulated expression were chosen. The qRT–PCR technology was used to analyze the expression of *PmbZIP* genes in different parts. The results in Figure 6 show that *PmbZIPs* were expressed in young needles, mature needles, roots, and stems but at different levels. Among these genes, *PmbZIP3*, *PmbZIP8*, and *PmbZIP20* were found to exhibit high expression levels in the roots. *PmbZIP23* was observed to have higher expression in young needles than in other tissues. *PmbZIP4* showed similar expression patterns in young needles, mature needles, and roots, which were slightly higher than those in the stems.

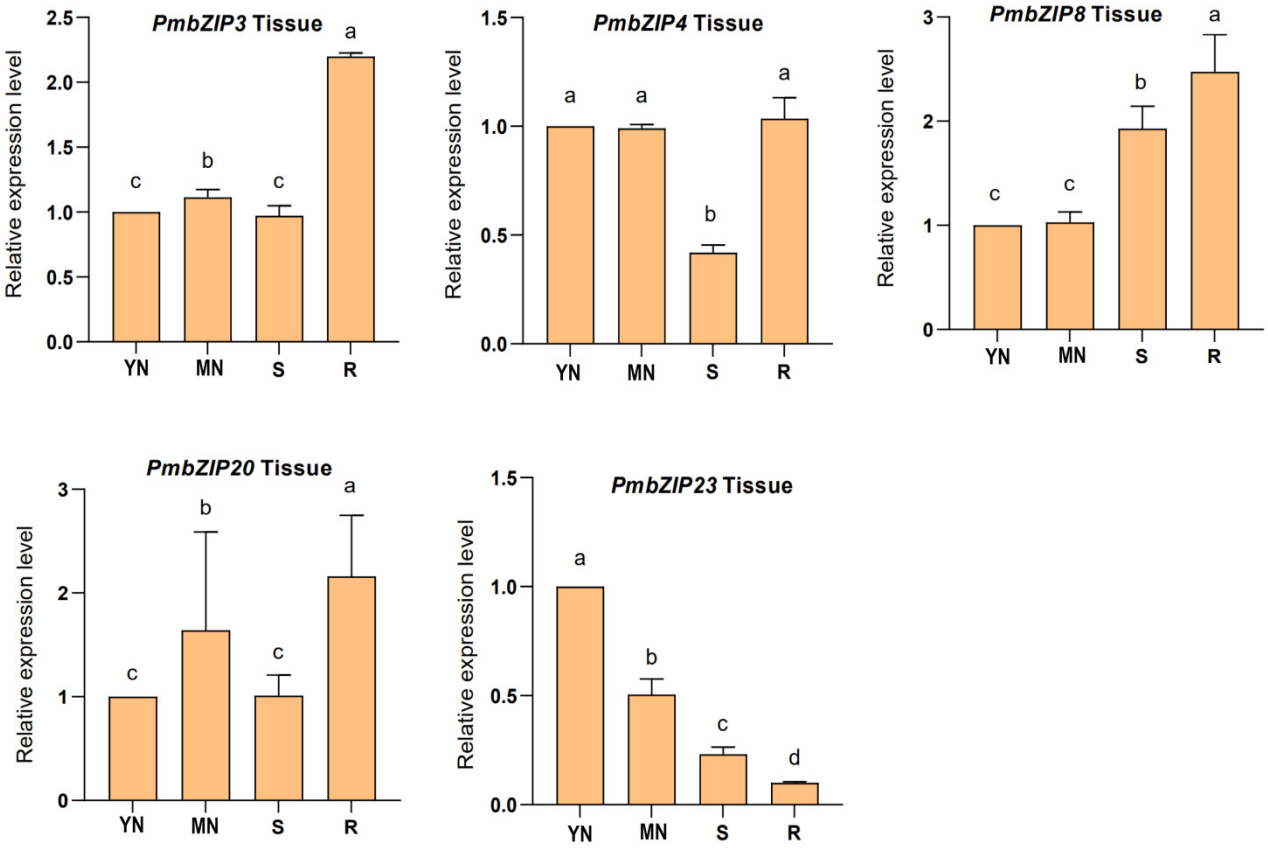

Figure 6. The expression levels of *PmbZIPs* in different tissues in *P. massoniana*. YN: young needles; MN: mature needles; S: stems; R: roots. The relative expression level is indicated as the mean ± standard deviation (SD). Different letters show significant differences at the 0.05 level with the Duncan method.

3.8. Expression Patterns of Selected PmbZIPs in Response to Different Treatments

The expression of the five *PmbZIP* genes after SA, MeJA, ETH, and H_2O_2 treatments is shown in Figure 7. After SA treatment, the expression of *PmbZIP4* and *PmbZIP8* smoothly increased at 12 h and subsequently decreased at 24 h. The expression level of *PmbZIP20* reached the highest level at 3 h and subsequently decreased. The expression of *PmbZIP3* and *PmbZIP23* decreased throughout the process. After MeJA treatment, the expression of *PmbZIP3* and *PmbZIP23* were downregulated. The expression levels of *PmbZIP4* and *PmbZIP8* sharply decreased at 3 h, then increased at 12 h, and subsequently decreased at 24 h. The expression of *PmbZIP20* was upregulated at 3 h and 12 h and then downregulated at 24 h. After ETH treatment, the expression trends of *PmbZIP4*, *PmbZIP8* and *PmbZIP20* were similar, and their expression levels increased throughout the whole process and peaked at 24 h. The expression trend of *PmbZIP3* slightly increased at 3 h and then decreased. However, the expression level of *PmbZIP23* continuously decreased. After H_2O_2 treatment, the expression levels of *PmbZIP4* and *PmbZIP8* sharply decreased at 3 h, then increased and reached the highest expression level at 24 h. The expression level of *PmbZIP3* first decreased and then smoothly increased. The expression of *PmbZIP20* was upregulated throughout the whole process. The expression of *PmbZIP23* presented a downregulated trend during the process.

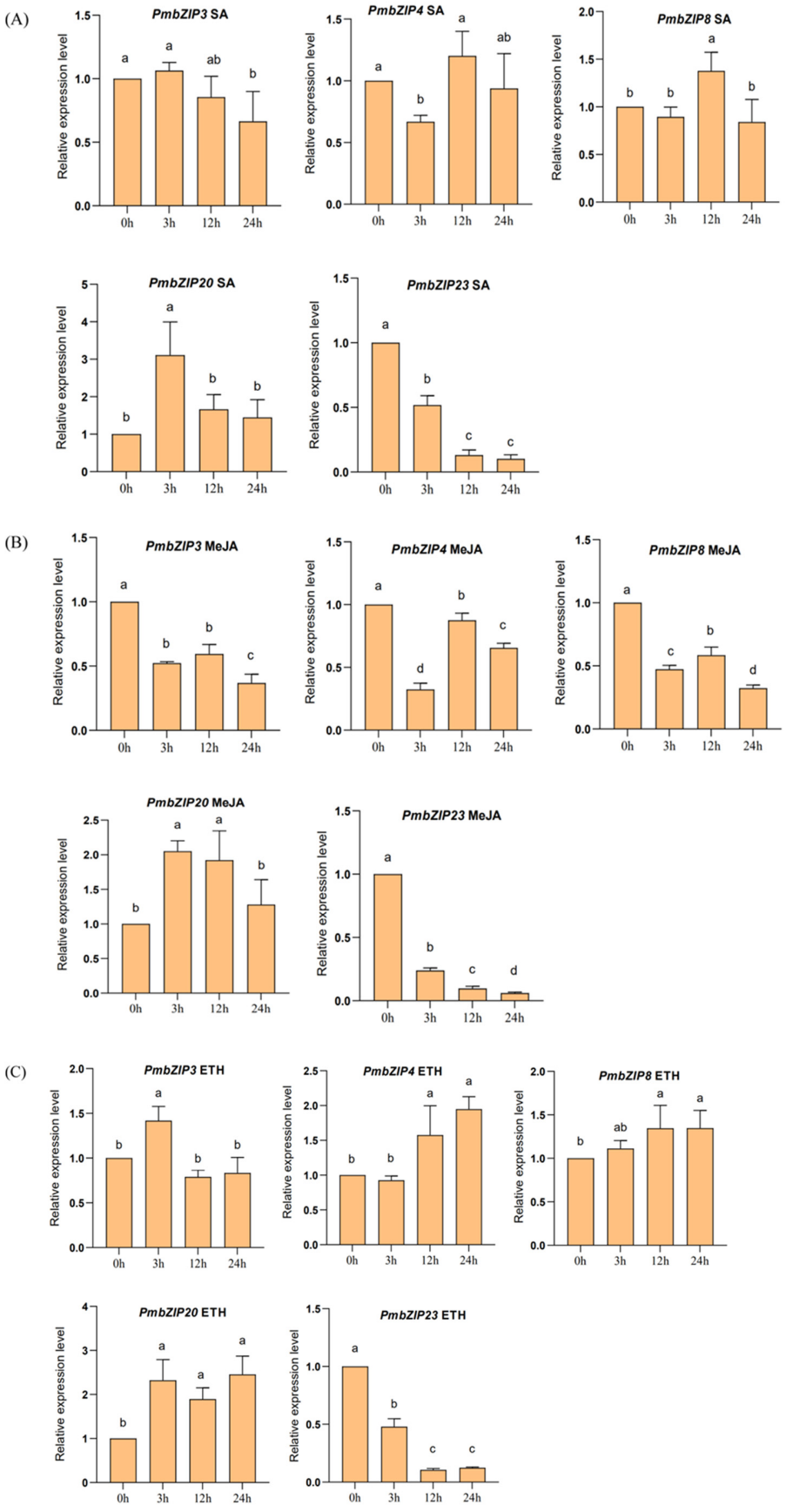

Figure 7. *Cont.*

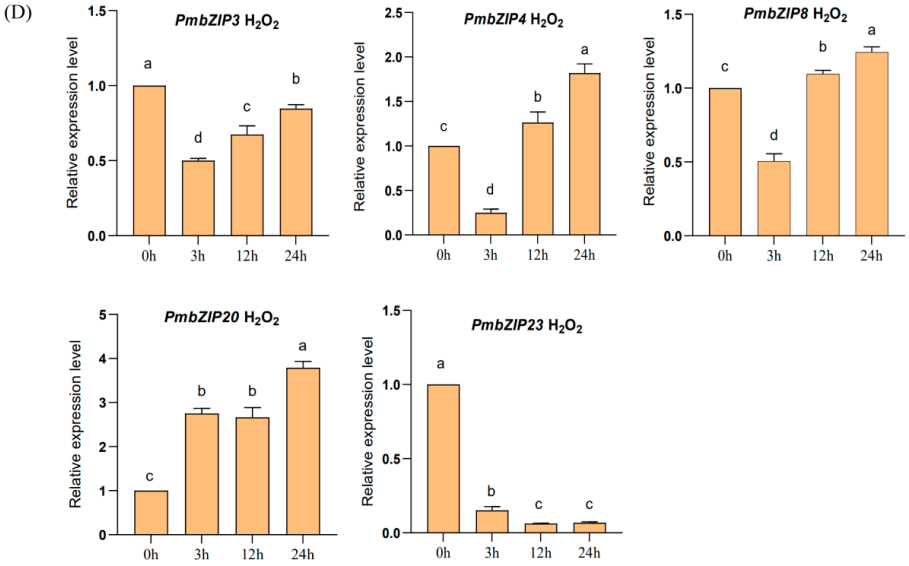

Figure 7. The expression levels of *PmbZIPs* in different treatments. (**A**) SA; (**B**) MeJA; (**C**) ETH; (**D**) H_2O_2. The relative expression level is indicated as the mean ± standard deviation (SD). Different letters show significant differences at the 0.05 level with the Duncan method.

3.9. Transcriptional Activity Assays of PmbZIPs

Furthermore, the transcriptional activity of these five PmbZIP proteins was determined. As shown in Figure 8, the yeast cells containing fusion vectors pGBKT7-PmbZIP3 and pGBKT7-PmbZIP8 could grow on SD/-Ade/-His/-Trp selected medium and appeared as blue spots after adding X-α-gal. The yeast cells containing fusion vectors pGBKT7-PmbZIP4, pGBKT7-PmbZIP20 and pGBKT7-PmbZIP23 could not grow on SD/-Ade/-His/-Trp selected medium and could not show blue spots on selected media containing X-α-gal, their growth state was consistent with the control (pGBKT7). The results showed that PmbZIP4, PmbZIP20 and PmbZIP23 proteins were transcriptional repressors, PmbZIP3 and PmbZIP8 proteins were transcriptional activators.

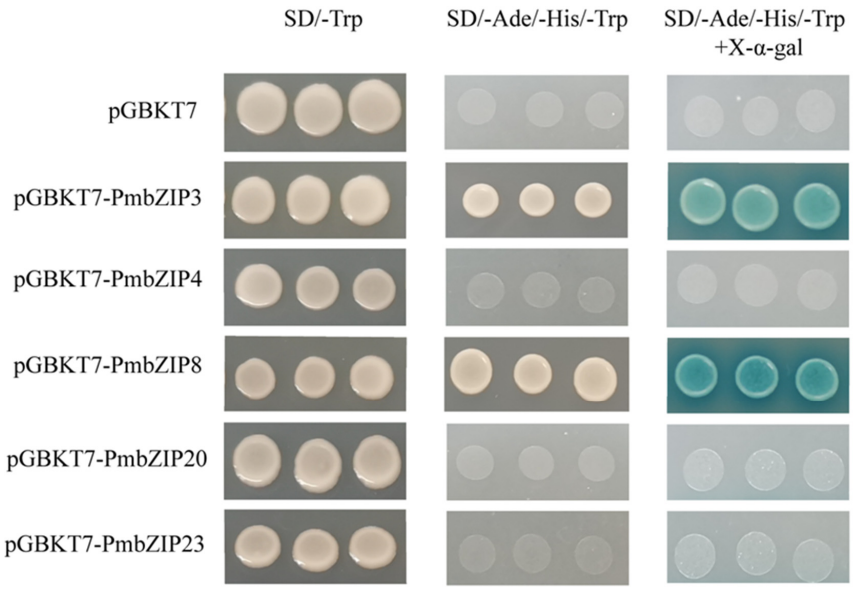

Figure 8. Transcriptional activity analysis of PmbZIP proteins. The growth state of the pGBKT7 (control), pGBKT7-PmbZIP3, pGBKT7-PmbZIP4, pGBKT7-PmbZIP8, pGBKT7-PmbZIP20 and pGBKT7-PmbZIP23 on SD/-Trp, SD/-Ade/-His/-Trp and SD/-Ade/-His/-Trp + X-α-gal medium.

4. Discussion

Relevant studies have shown that bZIPs play vital roles in many biological processes, including plant development, metabolism, and a variety of stresses [36,37]. The bZIP TFs have been found in *O. sativa* [38], *Elaeis guineensis* Jacq. [39], *Malus domestica* [14], *Brassica napus* L. [40], and many other species. For the first time, we systematically identified bZIP TFs from the four transcriptomes of *P. massoniana*. Moreover, the PmbZIP members were analyzed to determine evolutionary relationships, conserved domains, motif structures, transcriptional profiling, qRT–PCR expression patterns, subcellular localization, and transcriptional activity.

Fifty-five PmbZIP TFs were identified from the *P. massoniana* transcriptomes and renamed PmbZIP1-PmbZIP55. Almost all PmbZIP proteins had conserved structures of unchanged sequences (N-X7-R/K) and leucine zipper regions. In the unchanging N-X7-R basic region, arginine (R) and asparagine (N) are the most conserved sites. However, only one protein (PmbZIP33) had a mutation at the arginine (R) position, the residue of which was replaced by a tryptophan (T) residue, which is 1.8% of all proteins. A similar pattern was also observed in *Fusarium graminearum* and poplar [41,42]. A total of 55 PmbZIP TFs were divided into 11 groups, which is basically the same as that of *Arabidopsis* [7]. Interestingly, groups B, J and M did not contain *P. massoniana* bZIP members, indicating that some non-conserved bZIP members were probably lost in the process of evolution to fulfill the demand for growth. In a study of the tobacco bZIP family, it was also found that groups J and M did not contain NtbZIP TFs [35]. Moreover, eight PmbZIP members were classified into a new group of L, indicating that a separate group may have evolved, which may be related to its own characteristics. In a study of the jujube bZIP family, it was also found that some ZjbZIPs were discovered in new subfamilies [12]. These results were almost aligned with the results of the current study. Motif analysis showed that the types and numbers of motifs were broadly similar in the same group of most PmbZIP TFs, and the motifs were arranged in the same order, some groups also contained specific motifs, which firmly supported the evolutionary relationship, as well as group classification of PmbZIPs. These phenomena have been observed in olive [43], cassava [44], and grapevine [13]. Taken together, these findings indicated that PmbZIP TFs were conserved in structure.

The prediction of subcellular localization and transient transformation experiment showed that PmbZIPs are nucleoproteins; which is in accordance with the characteristics of tobacco bZIP TFs and the theory that TFs normally play a role in the nucleus [35].

Gene expression profiles are thought to be related to gene functions [45]. It has been reported that bZIP TFs participate in multiple stress resistance, and *P. massoniana* is easily attacked by pine wood nematodes [46,47]. Therefore, it is important to study the function of PmbZIPs in pine wood nematodes, and we analyzed the transcriptional profiles of PmbZIP family members via the pine wood nematode inoculation transcriptome. Within 35 d of pine wood nematode inoculation, the expression levels of many PmbZIP members significantly increased at 35 d, and a few increased separately at 3, 10 and 20 d. In addition, the overall expression trend of many genes first increased, then decreased and subsequently increased. These results indicated that *PmbZIP* genes could respond and positively regulate pine wood nematode infection, but their regulatory mechanisms were different and complex. Hence, this study laid a basic foundation for further study on the role of PmbZIPs in pine wood nematodes.

It has been found that the functions of some *bZIPs* are related to plant growth [48]. For instance, *AtbZIP11* (At4G34590.1) controls auxin-dependent primary root growth [49], and its homolog in *P. massoniana*, *PmbZIP20*, is highly expressed in roots, indicating that *PmbZIP20* may regulate root growth. *AtbZIP56* (At5G11260.1) promotes photomorphogenesis, chloroplast development and pigment accumulation [50]. The expression level of the *P. massoniana* homolog *PmbZIP23* in young leaves was higher than that in other tissues, which is consistent with the expression level of *AtbZIP56* promoting chloroplast synthesis. *AtbZIP68* (At1G32150.1) and *AtbZIP16* (At2G35530.1) are involved in the light response process [51]; the expression of the *P. massoniana* homologs *PmbZIP3* and *PmbZIP8* in the

roots was higher than that in other tissues, which may be related to photosynthate transport and accumulation in the roots. *AtbZIP46* (At1G68640.1) controls the formation of floral organ primordia [52], and its *P. massoniana* homolog, *PmbZIP4*, had a similar expression pattern in young leaves, mature leaves, and roots, implying that *PmbZIP4* may have similar functionality to *AtbZIP46* and could regulate organs development.

Relevant studies have shown that a number of bZIP members are involved in signal transduction of hormone synthesis pathways and respond to a variety of stresses [53]. SA, MeJA, ETH and H_2O_2 are important signaling molecules that are induced by environmental stimuli and play a key role in the response to stress [54,55]. In *Arabidopsis*, *AtbZIP11* promotes metabolic reprogramming under energy or nutrient starvation, resulting in metabolic adaptation and survival [49]; the expression of its homolog in *P. massoniana*, *PmbZIP20*, is upregulated after SA, MeJA, ETH, and H_2O_2 treatments, indicating that *PmbZIP20* may improve resistance to external stress through these signaling pathways. *AtbZIP56* is involved in various hormone signaling pathways that coordinate light and environmental signals [56]; the expression level of the *P. massoniana* homolog *PmbZIP23* was lower than that of the control after SA, MeJA, ETH, and H_2O_2 treatments, suggesting that there may be some functional differences between them in some respects. *AtbZIP16* and *AtbZIP68*, which are homologs in *P. massoniana*, *PmbZIP3* peaked at 3 h after ETH treatment, and *PmbZIP8* increased its expression levels after SA, ETH, and H_2O_2 treatments, suggesting that *PmbZIP3* and *PmbZIP8* were expressed under the induction of the treatments. *AtbZIP46* interacts with the main regulators of the plant pathogenic response, increasing plant survival capability under pathogen and biological stress [57]; in its *P. massoniana* homolog, *PmbZIP4*, the expression level always increased after ETH and H_2O_2 treatments, implying that *PmbZIP4* may be involved in regulating the signaling pathways to enhance plant resistance.

By observing the growth status of yeast cells containing pGBKT7-PmbZIP fusion vectors on nutrient deficiency medium. PmbZIP4, PmbZIP20 and PmbZIP23 proteins were unable to grow on the medium, indicating that they had no transcriptional activation activity and could not activate the expression of downstream reporter genes. Therefore, subsequent yeast two-hybrid assays could be carried out. PmbZIP3 and PmbZIP8 had transcriptional activation activity, suggesting that they could activate the expression of downstream reporter genes. They could also interact with other TFs to form transcription complexes that directly or indirectly regulate the expression of downstream genes. Transcriptional self-activation activity analysis will be more conducive to study the regulation mechanism of TFs [58].

In brief, the study systematically analyzed the bZIP TFs of *P. massoniana*. It not only helps to select appropriate representative genes for further study, but also contributes to understanding the molecular mechanism of bZIP TFs. Meanwhile, the identification and characteristic analysis of PmbZIP TFs provides insight into the biological functions of bZIPs in *P. massoniana.*

5. Conclusions

In this study, fifty-five bZIP TFs were identified from four *P. massoniana* transcriptomes. These TFs were divided into 11 groups, each TF contained conserved domain and motifs. Subcellular localization prediction showed that PmbZIPs were nuclear localization proteins, PmbZIP4 and PmbZIP20 were chosen to subcellular localization experiments, which showed that they were located in the nucleus. Based on the pine wood nematode inoculation transcriptome, it was found that 25 PmbZIPs could positively respond to pine wood nematodes stress. The qRT-PCR analyses were performed on seedlings of *P. massoniana* under SA, MeJA, ETH and H_2O_2 treatments, five representative genes namely, *PmbZIP3*, *PmbZIP4*, *PmbZIP8*, *PmbZIP20*, and *PmbZIP23,* were up-regulated or down-regulated to varying degrees in different time periods, indicating that the expression of *PmbZIP* genes may be induced by these exogenous exciters. Additionally, transcriptional activation activity showed that PmbZIP3 and PmbZIP8 were transcriptional activators; PmbZIP4,

PmbZIP20 and PmbZIP23 were transcriptional repressors. This study lays a theoretical foundation for the study of bZIP TFs and provides a potential strategy for the development of breeding related to pine wood nematode resistance in *P. massoniana*.

Supplementary Materials: The following supporting information can be downloaded at https://www.mdpi.com/article/10.3390/f14010155/s1: Table S1: Protein sequences; Table S2: Gene sequences; Table S3: Primer sequences; Table S4: FPKM values; Table S5: Physicochemical properties analysis; Table S6: Subcellular localization prediction; Figure S1: The eight motif logos identified within the bZIP family proteins.

Author Contributions: Conceptualization, M.Z.; software, M.Z. and S.Y.; methods, M.Z. and Q.H.; analysis, M.Z. and D.W.; investigation, M.Z., R.H.A., Z.H. and C.Z.; resources, M.Z. and P.Z.; writing—original draft preparation, M.Z. and P.Z.; writing—reviewing and editing, M.Z. and K.J. All authors have read and agreed to the published version of the manuscript.

Funding: This research was supported by the National Key R&D Program of China (2022YFD2200202) and the project was funded by the Priority Academic Program Development of Jiangsu Higher Education Institutions (PAPD).

Data Availability Statement: The data presented in this study are available in Supplementary Materials.

Conflicts of Interest: The authors declare that there are no conflict of interest.

References

1. Schwechheimer, C.; Bevan, M. The regulation of transcription factor activity in plants. *Trends Plant Sci.* **1998**, *3*, 378–383. [CrossRef]
2. Singh, K.B.; Foley, R.C.; Onate-Sanchez, L. Transcription factors in plant defense and stress responses. *Curr. Opin. Plant Biol.* **2002**, *5*, 430–436. [CrossRef] [PubMed]
3. Nakashima, K.; Takasaki, H.; Mizoi, J.; Shinozaki, K.; Yamaguchi-Shinozaki, K. NAC transcription factors in plant abiotic stress responses. *Biochim. Biophys. Acta* **2012**, *1819*, 97–103. [CrossRef] [PubMed]
4. Su, X.J.; Xia, Y.Y.; Jiang, W.B.; Shen, G.A.; Pang, Y.Z. *GbMYBR1* from *Ginkgo biloba* represses phenylpropanoid biosynthesis and trichome development in *Arabidopsis*. *Planta* **2020**, *252*, 68. [CrossRef] [PubMed]
5. Eulgem, T.; Somssich, I.E. Networks of WRKY transcription factors in defense signaling. *Curr. Opin. Plant Biol.* **2007**, *10*, 366–371. [CrossRef] [PubMed]
6. Thirugnanasambantham, K.; Durairaj, S.; Saravanan, S.; Karikalan, K.; Muralidaran, S.; Islam, V.I.H. Role of ethylene response transcription factor (ERF) and its regulation in response to stress encountered by plants. *Plant Mol. Biol. Rep.* **2014**, *33*, 347–357. [CrossRef]
7. Dröge-Laser, W.; Snoek, B.L.; Snel, B.; Weiste, C. The *Arabidopsis* bZIP transcription factor family-an update. *Curr. Opin. Plant Biol.* **2018**, *45*, 36–49. [CrossRef]
8. Wang, Z.J.; Zhu, J.; Yuan, W.Y.; Wang, Y.; Hu, P.P.; Jiao, C.Y.; Xia, H.M.; Wang, D.D.; Cai, Q.W.; Li, J.; et al. Genome-wide characterization of bZIP transcription factors and their expression patterns in response to drought and salinity stress in *Jatropha curcas*. *Int. J. Biol. Macromol.* **2021**, *181*, 1207–1223. [CrossRef]
9. Wang, J.Z.; Zhou, J.X.; Zhang, B.L.; Vanitha, J.; Ramachandran, S.; Jiang, S.Y. Genome-wide expansion and expression divergence of the basic leucine zipper transcription factors in higher plants with an emphasis on sorghum. *J. Integr. Plant Biol.* **2011**, *53*, 212–231. [CrossRef]
10. Zhao, J.; Guo, R.R.; Guo, C.L.; Hou, H.M.; Wang, X.P.; Gao, H. Evolutionary and expression analyses of the apple basic leucine zipper transcription factor family. *Front. Plant Sci.* **2016**, *7*, 376. [CrossRef]
11. Wei, K.F.; Chen, J.; Wang, Y.M.; Chen, Y.H.; Chen, S.X.; Lin, Y.N.; Pan, S.; Zhong, X.J.; Xie, D.X. Genome-wide analysis of bZIP-encoding genes in maize. *DNA Res.* **2012**, *19*, 463–476. [CrossRef] [PubMed]
12. Zhang, Y.; Gao, W.L.; Li, H.T.; Wang, Y.K.; Li, D.K.; Xue, C.L.; Liu, Z.G.; Liu, M.J.; Zhao, J. Genome-wide analysis of the bZIP gene family in Chinese jujube (*Ziziphus jujuba* Mill.). *BMC Genom.* **2020**, *21*, 483–496. [CrossRef] [PubMed]
13. Liu, J.Y.; Chen, N.N.; Chen, F.; Cai, B.; Dal Santo, S.; Tornielli, G.B.; Pezzotti, M.; Cheng, Z.M. Genome-wide analysis and expression profile of the bZIP transcription factor gene family in grapevine (*Vitis vinifera*). *BMC Genom.* **2014**, *15*, 281–298. [CrossRef]
14. Li, Y.Y.; Meng, D.; Li, M.J.; Cheng, L.L. Genome-wide identification and expression analysis of the bZIP gene family in apple (*Malus domestica*). *Tree Genet. Genomes* **2016**, *12*, 82. [CrossRef]
15. Yang, S.Q.; Xu, K.; Chen, S.J.; Li, T.F.; Xia, H.; Chen, L.; Liu, H.Y.; Luo, L.J. A stress-responsive bZIP transcription factor *OsbZIP62* improves drought and oxidative tolerance in rice. *BMC Plant Biol.* **2019**, *19*, 260–274. [CrossRef] [PubMed]
16. Xu, C.Y.; Cao, H.F.; Zhang, Q.Q.; Wang, H.Z.; Xin, W.; Xu, E.J.; Zhang, S.Q.; Yu, R.X.; Yu, D.X.; Hu, Y.X. Control of auxin-induced callus formation by bZIP59-LBD complex in *Arabidopsis* regeneration. *Nat. Plants* **2018**, *4*, 108–115. [CrossRef] [PubMed]

17. Van Leene, J.; Blomme, J.; Kulkarni, S.R.; Cannoot, B.; De Winne, N.; Eeckhout, D.; Persiau, G.; Van De Slijke, E.; Vercruysse, L.; Bossche, R.V.; et al. Functional characterization of the *Arabidopsis* transcription factor bZIP29 reveals its role in leaf and root development. *J. Exp. Bot.* **2016**, *67*, 5825–5840. [CrossRef] [PubMed]
18. Inaba, S.; Kurata, R.; Kobayashi, M.; Yamagishi, Y.; Mori, I.; Ogata, Y.; Fukao, Y. Identification of putative target genes of *bZIP19*, a transcription factor essential for *Arabidopsis* adaptation to Zn deficiency in roots. *Plant J.* **2015**, *84*, 323–334. [CrossRef]
19. Howell, S.H. Endoplasmic reticulum stress responses in plants. *Annu. Rev. Plant Biol.* **2013**, *64*, 477–499. [CrossRef]
20. Wang, L.P.; Fobert, P.R. *Arabidopsis* clade I TGA factors regulate apoplastic defences against the bacterial pathogen *Pseudomonas syringae* through endoplasmic reticulum-based processes. *PloS ONE* **2013**, *8*, e77378. [CrossRef]
21. Akagi, T.; Katayama-ikegami, A.; Kobayashi, S.; Sato, A.; Kono, A.; Yonemori, K. Seasonal abscisic acid signal and a basic leucine zipper transcription factor, *DkbZIP5*, regulate proanthocyanidin biosynthesis in persimmon fruit. *Plant Physiol.* **2012**, *158*, 1089–1102. [CrossRef] [PubMed]
22. Zhang, Y.Q.; Zheng, S.; Liu, Z.J.; Wang, L.G.; Bi, Y.R. Both *HY5* and *HYH* are necessary regulators for low temperature-induced anthocyanin accumulation in *Arabidopsis* seedlings. *J. Plant Physiol.* **2011**, *168*, 367–374. [CrossRef] [PubMed]
23. Fricke, J.; Hillebrand, A.; Twyman, R.M.; Pruefer, D.; Gronover, C.S. Abscisic acid-dependent regulation of small rubber particle protein gene expression in *Taraxacum brevicorniculatum* is mediated by *TbbZIP1*. *Plant Cell Physiol.* **2013**, *54*, 448–464. [CrossRef] [PubMed]
24. Shao, C.C.; Duan, H.L.; Ding, G.J.; Luo, X.Y.; Fu, Y.H.; Lou, Q. Physiological and biochemical dynamics of *Pinus massoniana* Lamb. seedlings under extreme drought stress and during recovery. *Forests* **2022**, *13*, 65–78. [CrossRef]
25. Keeling, C.I.; Bohlmann, J. Genes, enzymes and chemicals of terpenoid diversity in the constitutive and induced defence of conifers against insects and pathogens. *New Phytol.* **2006**, *170*, 657–675. [CrossRef]
26. Xiao, Y.C.; Ye, L.; Zhao, M.X.; Yan, C.Q.; Wang, W.; Huang, Q.S.; Liang, K.; Meng, B.H.; Ke, X. Two new sesquiterpene glycosides isolated from the fresh needles of *Pinus massoniana* Lamb. *Nat. Prod. Res.* **2017**, *31*, 341–346. [CrossRef]
27. Bohlmann, J. Pine terpenoid defences in the mountain pine beetle epidemic and in other conifer pest interactions: Specialized enemies are eating holes into a diverse, dynamic and durable defence system. *Tree Physiol.* **2012**, *32*, 943–945. [CrossRef]
28. Yu, Y.; Qian, Y.C.; Jiang, M.Y.; Xu, J.; Yang, J.T.; Zhang, T.Y.; Gou, L.P.; Pi, E.X. Regulation mechanisms of plant basic leucine zippers to various abiotic stresses. *Front. Plant Sci.* **2020**, *11*, 1258. [CrossRef]
29. Wu, F.; Sun, X.B.; Zou, B.Z.; Zhu, P.H.; Lin, N.Q.; Lin, J.Q.; Ji, K.S. Transcriptional analysis of Masson pine (*Pinus massoniana*) under high CO_2 stress. *Genes* **2019**, *10*, 804. [CrossRef]
30. Kumar, S.; Stecher, G.; Tamura, K. MEGA7: Molecular evolutionary genetics analysis version 7.0 for bigger datasets. *Mol. Biol. Evol.* **2016**, *33*, 1870–1874. [CrossRef]
31. Yang, Z.H. PAML 4: Phylogenetic analysis by maximum likelihood. *Mol. Biol. Evol.* **2007**, *24*, 1586–1591. [CrossRef] [PubMed]
32. Chen, C.J.; Chen, H.; Zhang, Y.; Thomas, H.R.; Frank, M.H.; He, Y.H.; Xia, R. TBtools: An integrative toolkit developed for interactive analyses of big biological data. *Mol. Plant* **2020**, *13*, 1194–1202. [CrossRef] [PubMed]
33. Zhu, P.H.; Ma, Y.Y.; Zhu, L.Z.; Chen, Y.; Li, R.; Ji, K.S. Selection of suitable reference genes in *Pinus massoniana* Lamb. under different abiotic stresses for qPCR normalization. *Forests* **2019**, *10*, 632–649. [CrossRef]
34. Livak, K.J.; Schmittgen, T.D. Analysis of relative gene expression data using real-time quantitative PCR and the 2 (T) (-Delta Delta C). *Methods* **2001**, *25*, 402–408. [CrossRef] [PubMed]
35. Li, Z.Y.; Chao, J.T.; Li, X.X.; Li, G.B.; Song, D.A.; Guo, Y.F.; Wu, X.R.; Liu, G.S. Systematic analysis of the bZIP family in tobacco and functional characterization of *NtbZIP62* involvement in salt stress. *Agronomy* **2021**, *11*, 148–164. [CrossRef]
36. Wang, Q.; Guo, C.; Li, Z.Y.; Sun, J.H.; Wang, D.; Xu, L.T.; Li, X.X.; Guo, Y.F. Identification and analysis of bZIP family genes in potato and their potential roles in stress responses. *Front. Plant Sci.* **2021**, *12*, 637343–637359. [CrossRef] [PubMed]
37. Das, P.; Lakra, N.; Nutan, K.K.; Singla-Pareek, S.L.; Pareek, A. A unique bZIP transcription factor imparting multiple stress tolerance in Rice. *Rice* **2019**, *12*, 58–74. [CrossRef] [PubMed]
38. Nijhawan, A.; Jain, M.; Tyagi, A.K.; Khurana, J.P. Genomic survey and gene expression analysis of the basic leucine zipper transcription factor family in rice. *Plant Physiol.* **2008**, *146*, 333–350. [CrossRef]
39. Zhou, L.X.; Yarra, R. Genome-wide identification and expression analysis of bZIP transcription factors in oil palm (*Elaeis guineensis* Jacq.) under abiotic stress. *Protoplasma* **2021**, *259*, 469–483. [CrossRef]
40. Zhou, Y.; Xu, D.X.; Jia, L.D.; Huang, X.H.; Ma, G.Q.; Wang, S.X.; Zhu, M.C.; Zhang, A.X.; Guan, M.W.; Lu, K.; et al. Genome-wide identification and structural analysis of bZIP transcription factor genes in *Brassica napus*. *Genes* **2017**, *8*, 288–311. [CrossRef]
41. Hussain, S.; Tai, B.W.; Hussain, A.; Jahan, I.; Yang, B.L.; Xing, F.G. Genome-wide identification and expression analysis of the basic leucine zipper (bZIP) transcription factor gene family in *Fusarium graminearum*. *Genes* **2022**, *13*, 607–627. [CrossRef] [PubMed]
42. Zhao, K.; Chen, S.; Yao, W.J.; Cheng, Z.H.; Zhou, B.R.; Jiang, T.B. Genome-wide analysis and expression profile of the bZIP gene family in poplar. *BMC Plant Biol.* **2021**, *21*, 122–137. [CrossRef] [PubMed]
43. Rong, S.Y.; Wu, Z.Y.; Cheng, Z.Z.; Zhang, S.; Liu, H.; Huang, Q.M. Genome-wide identification, evolutionary patterns, and expression analysis of bZIP gene family in olive (*Olea europaea* L.). *Genes* **2020**, *11*, 510–531. [CrossRef] [PubMed]
44. Hu, W.; Yang, H.B.; Yan, Y.; Wei, Y.X.; Tie, W.W.; Ding, Z.H.; Zuo, J.; Peng, M.; Li, K.M. Genome-wide characterization and analysis of bZIP transcription factor gene family related to abiotic stress in cassava. *Sci. Rep.* **2016**, *6*, 22783–22794. [CrossRef]
45. Liu, C.T.; Mao, B.G.; Ou, S.J.; Wang, W.; Liu, L.C.; Wu, Y.B.; Chu, C.C.; Wang, X.P. OsbZIP71, a bZIP transcription factor, confers salinity and drought tolerance in rice. *Plant Mol. Biol.* **2014**, *84*, 19–36. [CrossRef]

46. Wang, Z.; Wang, C.Y.; Fang, Z.M.; Zhang, D.L.; Liu, L.; Lee, M.R.; Li, Z.; Li, J.J.; Sung, C.K. Advances in research of pathogenic mechanism of pine wilt disease. *Afr. J. Microbiol. Res.* **2010**, *4*, 437–442.
47. Ying, S.; Zhang, D.F.; Fu, J.; Shi, Y.S.; Song, Y.C.; Wang, T.Y.; Li, Y. Cloning and characterization of a maize bZIP transcription factor, ZmbZIP72, confers drought and salt tolerance in transgenic *Arabidopsis*. *Planta* **2012**, *235*, 253–266. [CrossRef]
48. Lovisetto, A.; Guzzo, F.; Tadiello, A.; Confortin, E.; Pavanello, A.; Botton, A.; Casadoro, G. Characterization of a bZIP gene highly expressed during ripening of the peach fruit. *Plant Physiol. Biochem.* **2013**, *70*, 462–470. [CrossRef]
49. Weiste, C.; Pedrotti, L.; Selvanayagam, J.; Muralidhara, P.; Fröschel, C.; Novák, O.; Ljung, K.; Hanson, J.; Dröge-Laser, W. The *Arabidopsis* bZIP11 transcription factor links low-energy signalling to auxin-mediated control of primary root growth. *PLoS Genet.* **2017**, *13*, e1006607. [CrossRef]
50. Gangappa, S.N.; Botto, J.F. The multifaceted roles of HY5 in plant growth and development. *Mol. Plant* **2016**, *9*, 1353–1365. [CrossRef]
51. Shen, H.S.; Cao, K.M.; Wang, X.P. *AtbZIP16* and *AtbZIP68*, two new members of GBFs, can interact with other G group bZIPs in *Arabidopsis thaliana*. *BMB Rep.* **2008**, *41*, 132–138. [CrossRef] [PubMed]
52. Maier, A.T.; Stehling-Sun, S.; Offenburger, S.; Lohmann, J.U. The bZIP transcription factor PERIANTHIA: A multifunctional hub for meristem control. *Front. Plant Sci.* **2011**, *2*, 79–95. [CrossRef]
53. Lu, Z.C.; Qiu, W.M.; Jin, K.M.; Yu, M.; Han, X.J.; He, X.Y.; Wu, L.H.; Wu, C.; Zhuo, R.Y. Identification and analysis of bZIP family genes in *Sedum plumbizincicola* and their potential roles in response to cadmium stress. *Front. Plant Sci.* **2022**, *13*, 859386. [CrossRef] [PubMed]
54. Chen, Z.X.; Silva, H.; Klessig, D.F. Active oxygen species in the induction of plant systemic acquired resistance by salicylic acid. *Science* **1993**, *262*, 1883–1886. [CrossRef] [PubMed]
55. Costa, A.; Drago, I.; Behera, S.; Zottini, M.; Pizzo, P.; Schroeder, J.I.; Pozzan, T.; Lo Schiavo, F. H_2O_2 in plant peroxisomes: An in vivo analysis uncovers a $Ca^{(2+)}$-dependent scavenging system. *Plant J.* **2010**, *62*, 760–772. [CrossRef]
56. Li, Q.F.; He, J.X. BZR1 Interacts with HY5 to mediate brassinosteroid-and light-regulated cotyledon opening in *Arabidopsis* in darkness. *Mol. Plant* **2016**, *9*, 113–125. [CrossRef]
57. Gatz, C. From pioneers to team players: TGA transcription factors provide a molecular link between different stress pathways. *Mol. Plant Microbe Interact.* **2013**, *26*, 151–159. [CrossRef]
58. Zhang, K.; Wang, M.D.; Dong, D.; Hu, N.W.; Chao, Y.H.; Zeng, H.M. Construction of a cDNA library and self-activation assay of *KdSAHH* gene in deciduous yeast. *J. Grassl.* **2021**, *29*, 2135–2140.